CHEMISTRY OF MATERIALS
Article

Chem. Mater. **2010,** *22,* 255–260 255
DOI:10.1021/cm903058c

Covalently Bonded Polyaniline−TiO_2 Hybrids: A Facile Approach to Highly Stable Anodic Electrochromic Materials with Low Oxidation Potentials

Shanxin Xiong,[†] Si Lei Phua,[‡] Bruce S. Dunn,[§] Jan Ma,[†,‡] and Xuehong Lu*[,†,‡]

[†]*Temasek Laboratories, Nanyang Technological University, 50 Nanyang Drive, Singapore 637553,* [‡]*School of Materials Science and Engineering, Nanyang Technological University, 50 Nanyang Ave., Singapore 639798, and* [§]*Department of Materials Science and Engineering, California NanoScience Institute, University of California at Los Angeles, Los Angeles, California 90095-1595*

Received October 2, 2009. Revised Manuscript Received November 18, 2009

In this article, we report the synthesis, structures, morphologies, and electrochromic properties of covalently bonded polyaniline (PANI)−TiO_2 hybrids. The hybrids were synthesized via a sol−gel process, followed by oxidative polymerization, using a bifunctional compound to bridge the two phases. In comparison with PANI, the hybrids show significant enhancement in optical contrast and coloration efficiency. Furthermore, when covalently bonded to PANI, the TiO_2 nanodomains can act as electron acceptors, reducing the oxidation potential and band gap of PANI, and improving the long-term electrochromic stability.

Introduction

Conjugated polymers have been widely studied as electrochromic materials, because of their relatively high optical contrast and fast switching speeds, as well as reasonably good processability when doped with organic acids having long alkyl chains or polymeric organic acids.[1] In general, however, these polymers have poorer electrochemical stability than electrochromic metal oxides, thus limiting their usage in a variety of applications. To solve this problem, nanocomposites comprised of conjugated polymer matrices and metal-oxide nanostructures have been studied and several groups have demonstrated that such nanocomposites can exhibit higher optical contrast and faster switching speeds than the corresponding bulk metal oxides and provide better stability than the conjugated polymer matrices.[2] Furthermore, the fact that some metal oxides, such as TiO_2, can also act as electron acceptors[3] and form electron donor−acceptor pairs when interacting with a *p*-type conjugated polymer, raises the possibility that the changes induced by the incorporation of metal oxides may go well beyond simply compositional and morphological modifications.

Electrochromic properties of conjugated polymer/TiO_2 nanocomposites have been reported by several groups. Baek et al. reported that the optical contrast, coloration efficiency, and response time of poly(1,4-bis(2-[3′, 4′-ethylenedioxy] thienyl)-2-methoxy-5−2‴-ethylethylhexyl oxybenzene) (PBETH)/TiO_2 nanocomposites were improved significantly over that of the PBETH alone, because of the interaction of PBETH with the TiO_2 nanoparticles.[4] However, the nature of this interaction was not discussed. Ma et al. electrochemically polymerized 3-methylthiophene in nanoporous and mesoporous TiO_2 films to form poly(3-methylthiophene) (PMeT)/TiO_2 nanocomposites.[5] The good long-term stability of the electrochromic devices they fabricated was attributed to better adhesion of TiO_2 to the electrode. Wu et al. reported that, with the addition of TiO_2 nanorods, the optical contrast, coloration efficiency, and stability of poly-(4,4-dioctylcyclopenta[2,1-b:3,4-b′]-dithiophene (PDOCPDT) were enhanced significantly, because of the open morphology of the polymer created by the incorporation of TiO_2 nanorods.[6] In all of the previously described studies, TiO_2 was physically incorporated in the conjugated polymers without covalent bonding between

*Author to whom correspondence should be addressed. E-mail: asxhlu@ntu.edu.sg.

(1) (a) Jain, V.; Sahoo, R.; Mishra, S. P.; Sinha, J.; Montazami, R.; Yochum, H. M.; Heflin, J. R.; Kumar, A. *Macromolecules* **2009**, *42*, 135. (b) Celebi, S.; Balan, A.; Epik, B.; Baran, D.; Toppare, L. *Org. Electron.* **2009**, *10*, 631. (c) Wu, C.-G.; Lu, M.-I.; Chang, S.-J.; Wei, C.-S. *Adv. Funct. Mater.* **2007**, *17*, 1063. (d) Walczak, R. M.; Reynolds, J. R. *Adv. Mater.* **2006**, *18*, 1121. (e) Sapp, S. A.; Sotzing, G. A.; Reynolds, J. R. *Chem. Mater.* **1998**, *10*, 2101.
(2) (a) Xia, X. H.; Tu, J. P.; Zhang, J.; Huang, X. H.; Wang, X. L.; Zhang, W. K.; Huang, H. *Electrochem. Commun.* **2009**, *11*, 702. (b) Deepa, M.; Srivastava, A. K.; Sood, K. N.; Murugan, A. V. *J. Electrochem. Soc.* **2008**, *155*, D703. (c) Elzanowska, H.; Miasek, E.; Birss, V. I. *Electrochim. Acta* **2008**, *53*, 2706. (d) Avino, C.; Panero, S.; Scrosati, B. *J. Mater. Chem.* **1993**, *3*, 1259.
(3) (a) Al-Dmour, H.; Taylor, D. M. *Appl. Phys. Lett.* **2009**, *94*, 223309. (b) Günes, S.; Marjanovic, N.; Nedeljkovic, J. M.; Sariciftci, N. S. *Nanotechnology* **2008**, *19*, 424009. (c) Boucléab, J.; Ravirajanac, P.; Nelson, J. *J. Mater. Chem.* **2007**, *17*, 3141. (d) Berger, T.; Lana-Villarreal, T.; Monllor-Satoca, D.; Gómez, R. *Electrochem. Commun.* **2006**, *8*, 1713.
(4) Baek, J.; Kim, Y.; Oh, H.; Kim, E. *Curr. Appl. Phys.* **2008**, *9*, S110.
(5) Ma, L.; Li, Y.; Yu, X.; Zhu, N.; Yang, Q.; Noh, C. *J. Solid State Electrochem.* **2008**, *12*, 1503.
(6) Wu, C.; Lu, M.; Jhong, M. *J. Polym. Sci: Part B: Polym. Phys.* **2008**, *46*, 1121.

Published on Web 12/10/2009

Scheme 1. Synthesis Route of the PANI−TiO_2 Hybrids

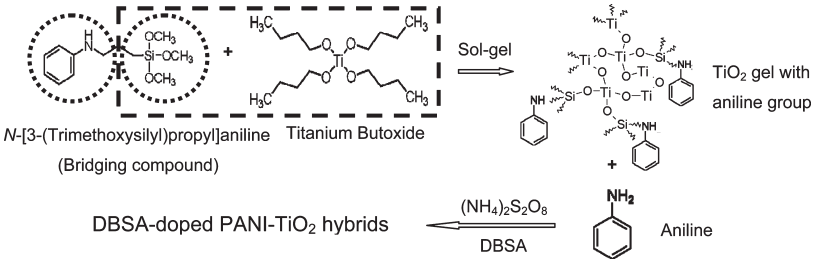

the organic and inorganic phases. Thus, the interactions between the two phases are likely to be weak, because of the relatively small interfacial areas caused by nanoparticle agglomeration and/or because of limited electron transport across the oxide/polymer interfaces. In the present work, our goal was to make interfacial interactions between the two components more prominent. We synthesized nanostructured polyaniline (PANI)−TiO_2 hybrid materials containing interfacial covalent bonds to enhance the interactions between the two components. These interactions influence the oxidation potentials and electrochemical stability of the resulting hybrid materials.

Experimental Section

Synthesis of PANI−TiO_2 Hybrids. All chemicals were purchased from Sigma−Aldrich and used as received. Xylene-soluble, dodecylbenzene sulfonic acid (DBSA)-doped PANI−TiO_2 hybrids were synthesized via a sol−gel process involving the reaction of titanium butoxide and a hybrid bridging compound, followed by oxidative polymerization of aniline in the presence of the hybrid gel and DBSA (see Scheme 1). In the first step for this synthesis, *N*-[3-(trimethoxysilyl)propyl]aniline (bridging compound)−TiO_2 cogel was prepared by adding 1.02 g (0.004 mol) of the bridging compound into a sol consisting of 39.1 g of ethanol, 8.5 g of titanium butoxide, 1.1 g of concentrated HNO_3, and 0.05 g of H_2O. This sol was aged for 48 h at room temperature. In the second step, emulsion polymerization of aniline (1.86 g, 0.02 mol) was performed in the presence of different amounts of the cogel (5.12, 11.3, and 19.43 g, respectively) in a water (80 g)/xylene (24 g) mixture using DBSA (9.8 g, 0.03 mol) and ammonium peroxydisulfate (1.37 g, 0.006 mol) as a surfactant/dopant and oxidant, respectively. This reaction was carried out for 24 h in a stirred water-ice bath. The hybrid solutions were then obtained by extracting the emulsion with xylene. The feed ratio of TiO_2 to aniline for these hybrids was 10/90, 20/80, and 30/70 (w/w), respectively. The three hybrid samples are identified as PANI−TiO_2-1, PANI−TiO_2-2, and PANI−TiO_2-3 in this paper.

We also synthesized several reference materials, to compare their properties to those of the hybrids. This includes the components of the hybrids (PANI and the TiO_2-bridging compound cogel), a TiO_2 gel, and also a PANI/TiO_2 composite material. The PANI was prepared using the same procedure as that of the hybrids but without the addition of the cogel. The TiO_2 gel was prepared using the same procedure as that of the cogel described earlier, except that no bridging compound was added into the sol. The PANI/TiO_2 composite was prepared using the same procedure as that of the hybrids, except that the cogel was replaced by the TiO_2 gel. For this composite material, the ratio of TiO_2 to aniline feed (by weight) was 20/80; this represents a composition that is nominally the same as that of PANI−TiO_2-2.

Fabrication of Thin Films and Electrochromic Devices. Xylene solutions of the PANI and hybrid materials were spin-coated onto indium tin oxide (ITO)-coated polyethylene terephthalate (PET) substrates (Sigma−Aldrich, 100 Ω/□) to form thin films. The TiO_2 films were formed by casting the sols onto these same substrates. The film thickness was measured using an Alpha-Step 500 profilometer. The single-active-layer electrochromic devices (cf. Figure S1a in the Supporting Information) used for spectro-electrochemical characterization were fabricated according to the methods described in our previous publication.[7] For the long-term stability studies, dual active-layer complementary electrochromic devices (cf. Figure S1b in the Supporting Information) were fabricated using the ITO-coated PET as the electrodes and an electrolyte consisting of poly(vinylidene fluoride) (PVDF)/1-butyl-3-methylimidazolium hexafluorophosphate (weight ratio of 1/1). The complementary electrochromic pairs were PANI/poly(3,4-ethylenedioxythiophene):poly(styrenesulfonate) (PEDOT:PSS) and PANI−TiO_2-2/PEDOT:PSS.

Characterization. Fourier transform infrared (FTIR) spectra of the materials were obtained on a Perkin−Elmer Model GX spectrometer, using the KBr pellet method. The powders used in the FTIR measurements were obtained by drying the xylene solutions of the materials and the gels under ambient conditions for several days. Thermogravimetric analysis (TGA) was performed using a TA Instruments Model Q500 instrument with a heating rate 10 °C/min over a temperature range of 40−750 °C in air. The ultraviolet−visible (UV−vis) spectra of the dilute solution in xylene were obtained using a Shimadzu Model 2501 spectrometer. Scanning electron microscopy (SEM) and energy-dispersive X-ray analysis (EDX) of the spin-coated films were performed using a JEOL Model JSM-6360 SEM system. Transmission electron microscopy (TEM) images were obtained using a JEOL Model JEM-2010 TEM system. The X-ray diffraction (XRD) measurements of the thin films were performed using a Shimadzu Model 6000 X-ray diffractometer with Cu Kα radiation. The cyclic voltammetry (CV) experiments were performed using platinum wire (99.99%, as a counterelectrode) and silver wire (99.9%, as a pseudo-reference electrode) in a 0.1 M $LiClO_4$/acetonitrile electrolyte solution. The pseudo-reference silver wire was calibrated vs. Fc/Fc^+ by dissolving ferrocene in the electrolyte solution and determining the $E_{1/2}$ value of the Fc/Fc^+ against the silver wire. In situ spectro-electrochemical properties of the devices were recorded using an Autolab PGSTAT30 potentiostat with the UV−vis spectrometer (Shimadzu Model 2501). The coloration efficiencies of the devices were measured

(7) (a) Xiong, S.; Xiao, Y.; Ma, J.; Zhang, L.; Lu, X. *Macromol. Rapid Commun.* **2007**, *28*, 281. (b) Jia, P.; Argun, A.; Xu, J.; Xiong, S.; Ma, J.; Hammond, P.; Lu, X. *Chem. Mater.* **2009**, *21*, 4434.

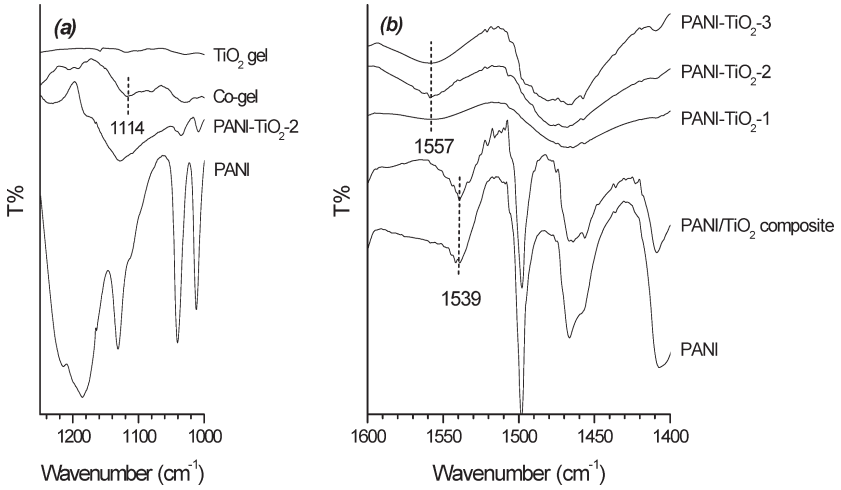

Figure 1. Fourier transform infrared (FTIR) spectra of the PANI−TiO_2 hybrids and associated reference materials: (a) the presence of a band at 1114 cm^{-1} for the cogel indicates that covalent bonding occurs between the TiO_2 and the bridging compound; (b) the blue shift in the band at 1539 cm^{-1} (quinoid rings) suggests that covalent bonding of the TiO_2 leads to increased doping of PANI.

Table 1. TiO_2 Contents, and Electrochemical and Electrochromic Properties, of the PANI−TiO_2 Hybrids and Reference Materials

	PANI	PANI−TiO_2-1	PANI−TiO_2-2	PANI−TiO_2-3	PANI/TiO_2 composite
feed TiO_2 content (wt %)[a]	0	2.46	5.38	8.88	5.38
measured TiO_2 content (wt %)[b]	0	2.71	5.14	7.92	2.07
anodic peak potential, $E_{p,a}$ (V)	0.39, 1.09	0.30, 0.86	0.29, 0.85	0.32, 0.66, 1.07[c]	0.41, 1.10
ABS λ_{max} (nm)[d]	737	750	768	772	746
band gap (eV)	1.54	1.50	1.39	1.41	1.52
contrast (ΔA) at λ_{max} (nm)[e]	0.43/660	0.49/640	0.53/645	0.51/635	0.25/790
coloration efficiency (cm^2/C)	165	175	207	150	81

[a] Calculated based on the assumption that the molar ratio of DBSA/PANI is 1:1 in the final product. [b] Obtained by subtracting the TGA residue of PANI from the residues of the hybrids. [c] The second oxidation peak is split into two peaks for PANI−TiO_2-3. [d] The wavelength of maximum absorbance (λ_{max}) measured in dilute solutions without applying external potential. [e] The λ_{max} value of the single-active-layer devices was measured at 1.5 V. The absorbance change of the devices at λ_{max} was determined by switching from −2.5 V to 1.5 V.

according to the method reported in ref 8. The switching behavior of the devices was determined at their wavelength of maximum absorbance (λ_{max}) with the potential stepped between −1.2 V and +1.2 V in step intervals of 20 s.

Results and Discussion

Synthesis and Morphology of PANI−TiO_2 Hybrids. PANI−TiO_2 hybrids were synthesized through the use of a bridging compound (see Scheme 1) to bond PANI and TiO_2 covalently, for the purpose of facilitating interactions between the two phases.

The formation of the covalent bonds between PANI and TiO_2 is indicated by FTIR spectra shown for a series of materials (see Figure 1). The reaction of the TiO_2 sol with the bridging compound creates a band at 1114 cm^{-1} for the cogel that corresponds to the asymmetrical vibration of the Si−O bond, where the O atom is directly linked to a Ti atom.[9] This new band suggests that covalent bonding is occurring. After polymerization, this band overlaps with the in-plane bending band of C−H in PANI; therefore, it is no longer possible to observe it clearly. Another important feature to note is the characteristic band of quinoid rings, which is observed at 1539 cm^{-1} for PANI and for the PANI/TiO_2 composite. For the hybrid material, however, this band is shifted significantly from 1539 cm^{-1} to 1557 cm^{-1}. This blue shift can be attributed to enhanced electron delocalization and the increased doping level of PANI caused by the electron-withdrawing feature of TiO_2. Such strong interactions occur only when the TiO_2 phase is covalently bonded to PANI. A final point to mention is that the FTIR results are consistent with the TiO_2 content of the materials synthesized. That is, in preparing the PANI/TiO_2 composite, it is apparent that much of the hydrophilic TiO_2 gel remains in the aqueous phase upon extraction with xylene, so that the TiO_2 content of the PANI/TiO_2 composite (as measured by TGA) is much lower than the feed value (see Table 1). In contrast, the TiO_2 contents of the hybrids are similar to the feed values, which indicate that covalently bonded TiO_2−PANI hybrids have been successfully synthesized.

In addition to the chemical differences shown in Table 1, the covalently bonded hybrids have very different morphologies from that of the composite. The TEM image of PANI−TiO_2-2 (see Figure 2a) shows that TiO_2-rich regions ~100 nm in length and ~30 nm in diameter are dispersed in the PANI matrix. The image at a higher magnification (see inset in Figure 2a) shows that such TiO_2-rich regions may consist of many small TiO_2 particles ~2 nm in size. In the PANI/TiO_2 composite, TiO_2 is not well-dispersed and the size of the TiO_2-rich

(8) Somani, P. R.; Radhakrishna, S. *Mater. Chem. Phys.* **2002**, *77*, 117.
(9) Shibli, S. M. A. A.; Mathai, S. *J. Mater. Sci: Mater. Med.* **2008**, *19*, 2971.

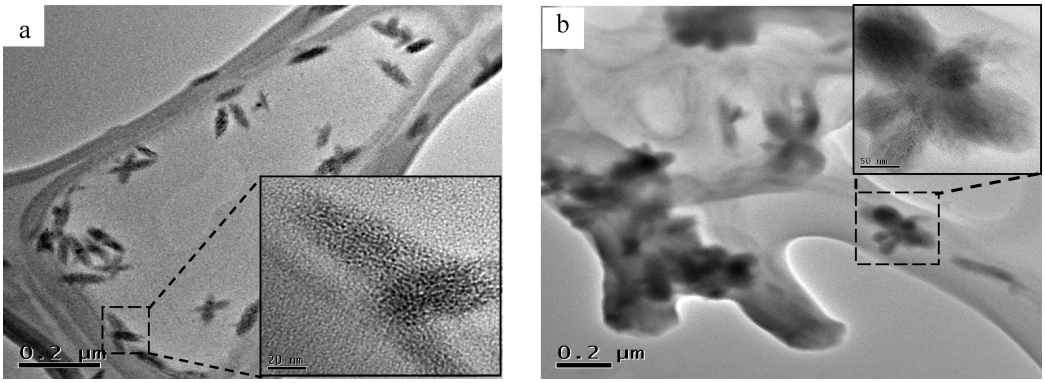

Figure 2. TEM images of (a) the PANI−TiO_2-2 hybrid and (b) the PANI/TiO_2 composite. Nanoscale TiO_2 particles are well-dispersed in the hybrid.

regions, which is several hundred nanometers, is much larger than that of the PANI−TiO_2-2 hybrid (see Figure 2b). In addition, the TiO_2-rich regions in the composite seem to be composed of a continuous TiO_2 phase instead of loose aggregates of smaller TiO_2 particles (see inset in Figure 2b). XRD studies reveal that the TiO_2 gel is completely amorphous (cf. Figure S2 in the Supporting Information). The hybrids and composite exhibit much lower crystallinity than PANI, indicating that the ordered packing of the PANI chains is disturbed by the presence of TiO_2-rich nanodomains.

Electrochemical and Spectro-electrochemical Properties of the Hybrids. Voltammetry sweeps are compared for PANI, TiO_2, and the PANI−TiO_2 hybrid materials in Figure 3. The absence of any peak for the TiO_2 film indicates that this material is not redox active in the potential range studied. PANI exhibits two oxidation peaks, at 0.39 and 1.09 V, which can be assigned to the leucoemeraldine base (LEB)-to-emeraldine salt (ES) and the ES-to-pernigraniline base (PNB) transitions, respectively, and two reduction peaks (at 0.76 V and −0.05 V) for the reverse transitions.[10] The CV voltammogram of the composite closely resembles that of PANI (cf. Figure S3 in the Supporting Information). Note that, in comparison with PANI and the composite, the oxidation peak potentials for all the PANI−TiO_2 hybrids are reduced significantly, and that the magnitude of the peak potential shift increases with the amount TiO_2 in the hybrids (see Table 1). For example, the ES-to-PNB transition decreases from 1.09 V for PANI to 0.86 V for PANI−TiO_2-2 and 0.66 V for PANI−TiO_2-3. We propose that the reason for the decrease in the oxidation potentials for the hybrids is that the electron donor (PANI)−acceptor (TiO_2) interaction causes a decrease in the energy of the highest occupied molecular orbital (HOMO) and ionization potential of PANI, thus enabling PANI to be oxidized at a lower potential. This feature is also shown by the lower band gap of the hybrids, compared to PANI and the PANI/TiO_2 composite (see Table 1), as calculated from the UV−vis spectra (cf. Figure S4 in the Supporting Information).[11] This behavior is consistent with similar phenomena observed

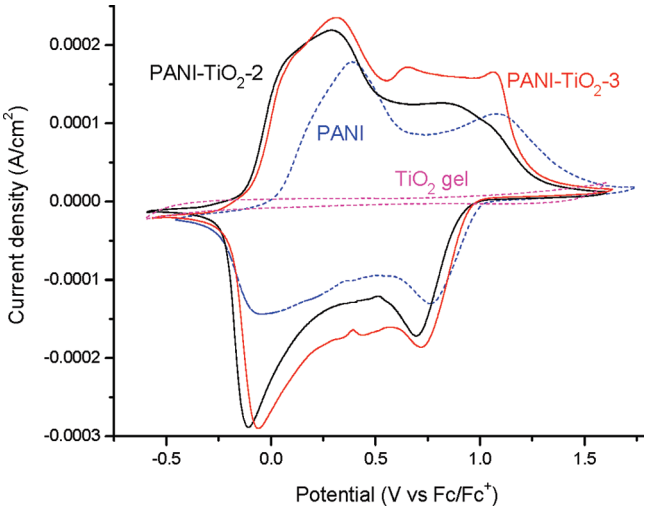

Figure 3. Cyclic voltammograms for the TiO_2 gel, PANI, and the PANI−TiO_2-2 and PANI−TiO_2-3 hybrids. The oxidation peak potentials for the hybrids are much lower than that of PANI. The experiments used 0.1 M $LiClO_4$ in acetonitrile as the electrolyte and a scan rate of 10 mV/s ,with platinum wire as the counterelectrode and silver wire as the pseudo-reference electrode.

in donor−acceptor-type organic electrochromic polymers.[12] Furthermore, with the highest TiO_2-containing hybrid (PANI−TiO_2-3), an additional peak becomes evident at the most anodic potentials, suggesting that the hybrids contain two active components: one is PANI covalently bonded with TiO_2, and the other is PANI not bonded with TiO_2.

We also investigated the effect of electron donor−acceptor interaction between PANI and TiO_2 in two different types of electrochromic devices (cf. Figure S1 in the Supporting Information). First, we constructed single-layer electrochromic devices, in which we directly compared the electrochromic responses of PANI and the PANI−TiO_2-2 hybrid, as shown in Figures 4a and 4b, respectively. Upon increasing the potential from −2.5 V to 0 V and then to 1.5 V, the color of the both devices changes from greenish yellow to green and then to sky blue. At 2.5 V, however, the color of the PANI device is

(10) Shreepathi, S.; Holze, R. *Chem. Mater.* **2005**, *17*, 4078.
(11) Yakuphanoglu, F.; Sekerci, M.; Evin, E. *Physica B* **2006**, *382*, 21.
(12) (a) Algi, F.; Cihaner, A. *Org. Electron.* **2009**, *10*, 253. (b) Gunbas, G. E.; Camurlu, P.; Akhmedov, İ. M.; Tanyeli, C.; Önal, A. M.; Toppare, L. *J. Electroanal. Chem.* **2008**, *615*, 75. (c) Steckler, T. T.; Abboud, K. A.; Craps, M.; Rinzler, A. G.; Reynolds, J. R. *Chem. Commun.* **2007**, *46*, 4904.

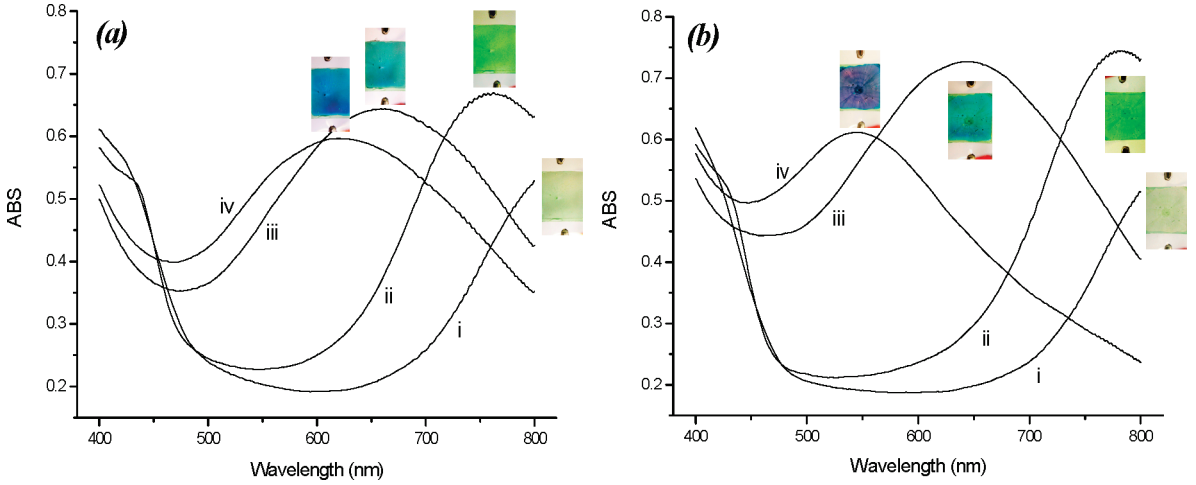

Figure 4. Absorption spectra in the visible range for electrochromic devices with (a) PANI and (b) PANI−TiO_2-2 as the electrochromic layer, respectively. The absorption curves were obtained at potentials of −2.5 V (curve i), 0 V (curve ii), 1.5 V (curve iii), and 2.5 V (curve iv). The colors of the devices at the various potentials are shown.

blue, while that of the PANI−TiO_2-2 device is purple, indicating that oxidation has progressed further in the hybrid than in the PANI. Furthermore, as the TiO_2 content increases, the wavelength of maximum absorbance (λ_{max}) at +1.5 V is blue-shifted from 660 nm for PANI to 640 nm for PANI−TiO_2-1 and PANI−TiO_2-2, and 635 nm for PANI−TiO_2-3 (see Table 1), suggesting that PANI chains in the hybrids become increasingly easier to oxidize. This behavior is consistent with the cyclic voltammetry observation that the oxidation peak potentials for the hybrids decrease as the TiO_2 content increases.

We also characterized two other properties that are commonly investigated with electrochromic films: optical contrast and coloration efficiency.[13] The PANI−TiO_2 hybrid material exhibits better properties than either PANI or the PANI/TiO_2 composite (see Table 1). The improvement compared to PANI occurs because of the lower crystallinity of the hybrid, which is an effect that has been discussed previously.[7] Although the TiO_2 phase in the potential range studied (cf. Figure S5 in the Supporting Information), without covalent bonding, is electrochromically inactive, the diffusive reflectance caused by the poor dispersion of the TiO_2 phase decreases the transparency of the electrochromic film. Such phase separation also explains why hybrid materials exhibit far better coloration efficiencies (CEs), compared to the composite. Interestingly, an increase in the TiO_2 content of the hybrid material leads to a better CE, although at the highest TiO_2 content (i.e., PANI−TiO_2-3), micrometer-level phase separation occurs (cf. Figure S6 in the Supporting Information), causing a decrease in the CE values of the hybrid film.

We also investigated complementary devices which incorporate commercial PEDOT:PSS as the ion storage layer and use a highly stable ionic liquid in a polar polymer host as the electrolyte (cf. Figure S1b in the Supporting Information). The focus of these experiments was to compare the long-term electrochemical stability of the PANI−TiO_2-2 hybrid to that of the PANI. For the first 20 000 cycles or so (see Figure 5), the PANI/PEDOT device exhibits good contrast between the bleached and colored states. The slow increase in the absorbance of the bleached state, which occurs upon cycling, indicates that, in each cycle, a small portion of oxidized PANI chains could not be reduced back to the LEB state, because of hydrolysis at the high oxidation level.[14] After ~20 000 cycles, however, the absorbance in the bleached state increases sharply and the contrast declines to 10% of its initial value at 34 000 cycles. It is striking to note that the contrast of the PANI−TiO_2-2/PEDOT device does not show appreciable decay after 50 000 cycles of switching. We attribute the high electrochromic stability of the

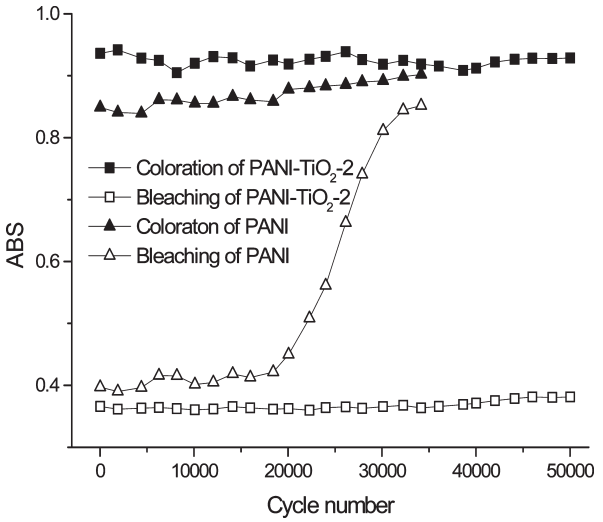

Figure 5. Absorbance of the PANI/PEDOT and PANI−TiO_2-2/PEDOT complementary devices at their colored and bleached states, as a function of the number of switching cycles. Absorption was measured at 680 nm for the PANI/PEDOT devices. The corresponding wavelength for the PANI−TiO_2-2/PEDOT device was 650 nm.

(13) Li, M.; Sheynin, Y.; Patra, A.; Bendikov, M. *Chem. Mater.* **2009**, *21*, 2482.

(14) Salamifar, E.; Mehrgardi, M. A.; Mousavi, M. F. *Electrochim. Acta* **2009**, *54*, 4638.

hybrid to the prominent donor−acceptor interaction between PANI and TiO_2, which stabilizes semiquinone radicals during the redox process of PANI.[15]

Conclusions

A series of novel polyaniline (PANI)−TiO_2 hybrid electrochromic materials are readily synthesized using the sol−gel process, followed by oxidative polymerization. With the aid of the bridge compound used in the sol−gel process, TiO_2 is dispersed in PANI at the nanometer level and covalent bonds are formed between the organic and inorganic phases. The electron donor (PANI)−acceptor (TiO_2) interactions cause a decrease in the highest occupied molecular orbital (HOMO) energy, which enables PANI to be oxidized at a lower potential and leads to improved electrochemical stability. In addition, the lower crystallinity and better transparency of the PANI−TiO_2 hybrid leads to electrochromic devices with improved optical contrast and coloration efficiency, compared to PANI or PANI composites. We believe that the hybrid approach may be applied to other conjugated polymer/metal oxide hybrid systems and, thus, has significant impact on the applications of conjugated polymers in electrochromic and electrochemical devices.

Supporting Information Available: Schematics showing configurations of the electrocrhomic devices, X-ray diffraction patterns, cyclic voltammograms and UV−vis spectra of the hybrids and reference materials, visible spectra of the electrochromic devices using the TiO_2 and PANI/TiO_2 composite as the electrochromic layer, respectively, at different potentials, and SEM micrographs and EDX spectra of the hybrid and composite thin films. This information is available free of charge via the Internet at http://pubs.acs.org/.

(15) Ito, S.; Kubo, T.; Morita, N.; Ikoma, T.; Tero-Kubota, S.; Tajiri, A. *J. Org. Chem.* **2003**, *68*, 9753.